VIA MEDICA

Nuclear Medicine Review 2022, 25, 1: 37–46
DOI: 10.5603/NMR.a2022.0008

ISSN 1506–9680, e-ISSN 1644–4345

Original

Optimized method for normal range estimation of standardized uptake values (SUVmax, SUVmean) in liver SPECT/CT images with somatostatin analog [^{99m}Tc]-HYNIC-TOC (Tektrotyd)

Hanna Piwowarska-Bilska, Sara Kurkowska, Bozena Birkenfeld
Department of Nuclear Medicine, Pomeranian Medical University, Szczecin, Poland

[Received 12 XI 2021; Accepted 29 XII 2021]

Abstract

Background: ^{99m}Tc-hydrazinonicotinyl-Tyr3-octreotide ([^{99m}Tc]-HYNIC-TOC [Tektrotyd]) is a radiopharmaceutical used for the diagnosis of lesions with overexpression of somatostatin receptors. The purpose of this study was to optimize the method and estimate normal ranges for standardized uptake values of Tektrotyd in healthy livers.

Material and methods: An analysis of standardized uptake value (SUVs) normal ranges was performed for images acquired in a selected "healthy group" of 42 patients evaluated for neuroendocrin tumors. The "pathological group" comprised 20 patients with liver lesions detected by scintigraphic imaging. Normal ranges for radiopharmaceutical uptake values were estimated based on the quantitative analysis of images acquired with a GE Healthcare NM/CT 850 gamma camera.

Results: The method for healthy liver segmentation in single photon emission computed tomography/computed tomography (SPECT/CT) was optimized. The normal range of SUVs for the liver was: standardized uptake value body weight **(**SUVbw) max [5.2–14.0] g/mL and standardized uptake value lean body mass (SUVlbm) [3.5–9.5] g/mL. The relative standard error (relative SE) of activity concentration estimated in the phantom study for the largest hot spheres was: φ = 37 mm — 5.9%, φ = 28 mm — 7.1%, φ = 22 mm — 11.4%, and φ = 17 mm — 22%.

Conclusions: Segmentation in the mid-coronal computed tomography (CT) image, at one-fourth of the height of the liver measured from the top, with a medium-sized volume of interest (VOI) outlined on a given transverse SPECT slice was regarded as the optimal method for estimating normal ranges for standardized uptake values. It is necessary to standardize quantification methods in the SPECT/CT studies. Our work is a step forward in obtaining standardization of SPECT/CT SUV calculation methods. Calculations for radiopharmaceutical uptake in tumors with volumes smaller than 5 mL are biased with a significant measurement error.

KEY words: quantitative SPECT/CT; SUV; standardized uptake value; [^{99m}Tc]-HYNIC-TOC; Tektrotyd

Nucl Med Rev 2022; 25, 1: 37–46

Correspondence to: Hanna Piwowarska-Bilska,
Department of Nuclear Medicine, Pomeranian Medical University,
Unii Lubelskiej 1, 71-344 Szczecin, Poland
e-mail: hanna.piwowarska@pum.edu.pl

Introduction

SPECT/CT and positron emission tomography/computed tomography (PET/CT) imaging with radiolabeled analogues of somatostatin plays an important role in the diagnosis and monitoring of patients with neuroendocrine tumors (NET). These techniques offer additional metabolic information and higher specificity than conventional magnetic resonance imaging (MRI) or CT [1, 2]. Radioisotope studies of somatostatin receptors are used for diagnostic purposes and in the process of qualifying patients for peptide receptor radionuclide therapy (PRRT). The somatostatin analog [^{99m}Tc]-HYNIC-TOC (Tektrotyd), manufactured in Poland, has been used for over a decade in many European countries for imaging NET with SPECT/CT. This radiopharmaceutical is characterized by a high affinity for somatostatin receptors type 2 (SSTR2), a lower affinity for SSTR3 and SSTR5, optimal physical parameters, and biodistribution. In 2003 Gabriel et al. [3] reported a higher sensitivity of [^{99m}Tc]-HYNIC-TOC as compared to ^{111}Indium-diethylenetriaminepentaacetic acid-d-phenylalanine-octreotide ([^{111}In]-DTPA-octreotide [Octreoscan]) for the detection of neuroendocrine tumors. Tektrotyd has many advantages with respect to Octreoscan, including better physical characteristics of [^{99m}Tc] compared to [^{111}In], which makes it more suitable for SPECT/CT imaging; shorter half-life; lower radiation burden; lower physiological liver and bowel uptake [4]. Therefore, Tektrotyd is a good alternative to [^{68}Ga]-DOTA-Peptide in medical centers where PET/CT or [^{68}Ge]/[^{68}Ga] generators are not available [5, 6, 7].

In PET/CT imaging, the quantitative assessment of uptake by NET measured by SUV is a standard procedure [8, 9]. Modern SPECT/CT systems offer quantitative imaging. Physicians referring their patients for imaging with [^{99m}Tc]-HYNIC-TOC expect quantitative data on radionuclide uptake by tumors. However, standardized uptake values (SUVs) when presented without an estimated normal range for SUV do not provide any important or conclusive diagnostic information.

In clinical practice, the qualification of patients for PRRT with somatostatin analogs is based, among others, on the assessment of the intensity of uptake in tumors with a semiquantitative visual scoring system, known as Krenning score, which consists of a scale from 0 to 4 and uses the liver and spleen as reference organs [10]. Moreover, it has been found that the maximum standardized uptake value (SUVmax) is strongly correlated with Krenning score [11]. Quantitative nuclear medicine is diagnostically and therapeutically more effective than qualitative because visual analysis of SPECT/CT images can be subjective and not repeatable [12].

The primary purpose of this study was to optimize the method for the segmentation of healthy liver in order to estimate normal ranges for SUV. The detailed aims of the study were to estimate normal ranges for standardized uptake values (SUVmax, mean standardized uptake value [SUVmean]) in SPECT/CT images of healthy liver acquired using Tektrotyd and a GE Healthcare NM/CT 850 gamma camera, and to estimate the accuracy of SUV measurements performed in a body phantom.

In addition to the absolute normal standardized uptake values of Tektrotyd, we also calculated the relative ranges for the following ratios: SUV spleen/SUV liver and SUV liver/SUV gluteus medius which may help to overcome the problem of the individual presence of somatostatin receptors in healthy patients.

Material and methods

Patient images

An analysis of normal ranges for SUV was performed for images acquired in a selected "healthy group" of 42 patients (29 men, 13 women, mean age 60 years) evaluated for NET. They had a physiological liver distribution of Tektrotyd, as well as normal results of selected biochemical liver tests (aspartate aminotransferase test [AST] and alanine aminotransferase test [ALT]) and normal results of CT or MRI scan of the abdomen. The "pathological group" comprised 20 patients (13 men and 7 women, mean age 61 years) with hot liver lesions detected by scintigraphy. In this group, 58 hot lesions in the livers were described. All of these patients were diagnosed before SPECT/CT examinations, based on the biopsy results of the primary lesion. Histopathological examination revealed NET of the gastrointestinal tract in 18 of these patients and the carcinoid of the lung in 2 other patients. SPECT/CT was performed to assess the severity of the disease.

Patient SPECT/CT scans were acquired 2–5 hours following the injection of 483–765 Megabecquerel (MBq) of the radiopharmaceutical. Syringe activity for each patient was measured before and after the injection of Tektrotyd. SUVs in SPECT/CT images were calculated with the Q.Metrix option of Xeleris 4.0 software.

Normal ranges for radiopharmaceutical uptake values were estimated based on the quantitative analysis of images acquired with a GE Healthcare NM/CT 850 gamma camera. The following SPECT/CT acquisition parameters were used: low energy high resolution (LEHR) collimator, 120 projections, projection time 20 s, matrix 128 x 128, dual-energy windows: emission 126.5–154.6 keV, scatter 114.0–126.0 keV, and low dose CT after SPECT mode. The reconstruction parameters were: 5 iterations and 15 subsets, without a reconstruction filter. Segmentation of regions of interest (ROIs) in patient images and phantom images was performed at a 50% cut-off threshold for the background. The volumes of interest (VOIs) were drawn in the reconstructed SPECT images by manually adjusting the threshold of an isocontour such that the VOI boundaries coincided with the boundaries of the fused CT image.

Optimization of the method for estimating normal range for SUV in the liver

The quantification of the images began with the clinical optimization of the liver segmentation method in the images of healthy subjects.

1) Segmentation of the entire area of the liver without the regions of extrahepatic bile ducts

During the quantitative analysis, SPECT and CT images of the same liver slices were displayed. Correct liver segmentation in SPECT slices was anatomically monitored on the corresponding CT slices. The segmentation technique involved the outlining of the entire liver area, without the extrahepatic bile ducts, on individual transverse slices (Fig. 1). ROIs were outlined on every fourth SPECT transverse slice. As a result, VOIs were created on 3D images covering a considerable portion of the liver, with a mean volume of 1296 ± 299 mL.

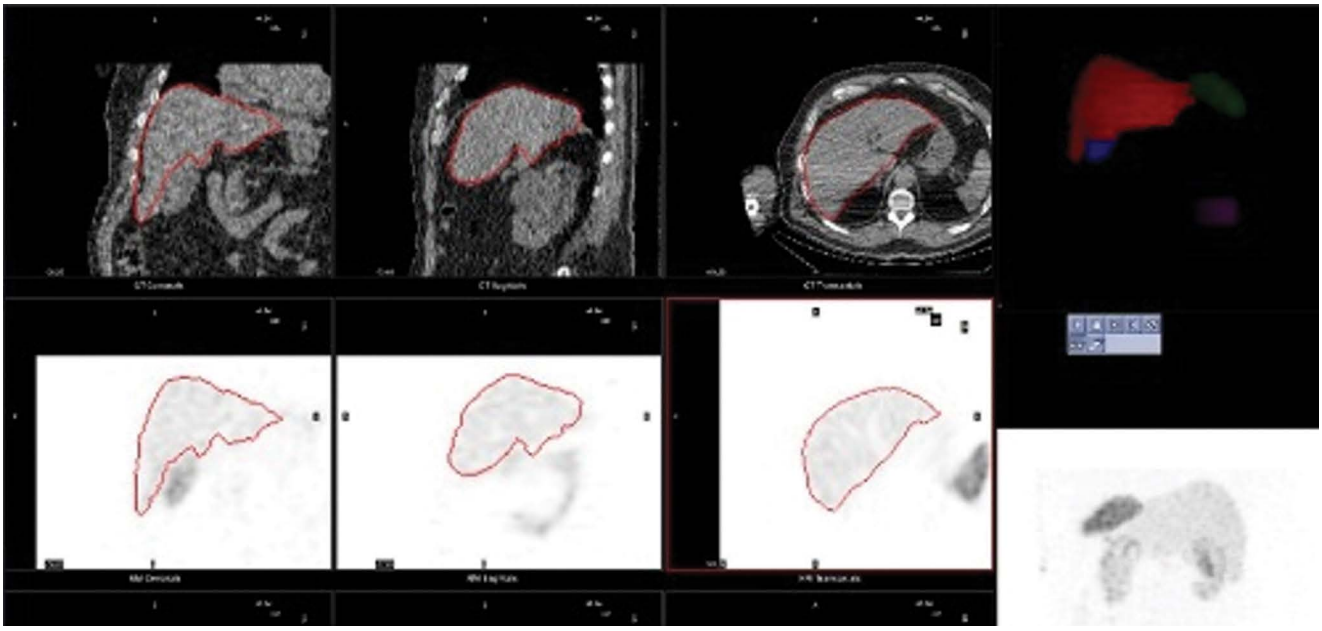

Figure 1. Liver segmentation method 1 with Q.Metrix option of Xeleris 4.0 software

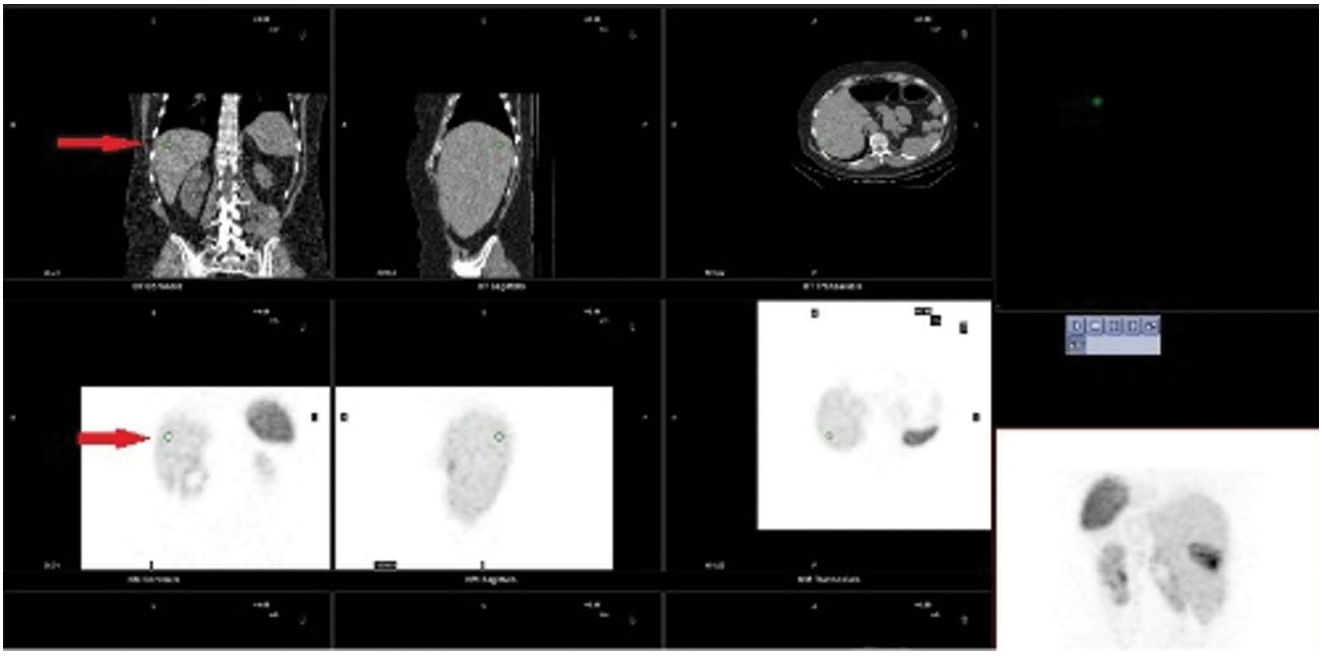

Figure 2. Small liver volume of interest (VOI) — segmentation method 2

2) Method for the segmentation of a small liver VOI on the established slice

A CT slice corresponding to the SPECT slice showing the Th11 and Th12 vertebra was displayed. A liver fragment of the mean volume 2.5 ± 0.7 mL was segmented at the level of the intervertebral disc between Th11 and Th12 (Fig. 2), within peripheral localization of liver segments V and VI.

3) Segmentation method for the medium-sized liver VOI at 1/4 of the height of the liver (measured from the top)

Segmentation was performed as follows: in the mid-coronal CT image of the patient's liver, one-fourth of the height of the liver from the top was determined. Then, on the given transverse SPECT slice, the ROI outlining the liver was selected (Fig. 3). The mean size of the VOI created with this method was 31.1 ± 7.7 mL within liver segments VII and VIII.

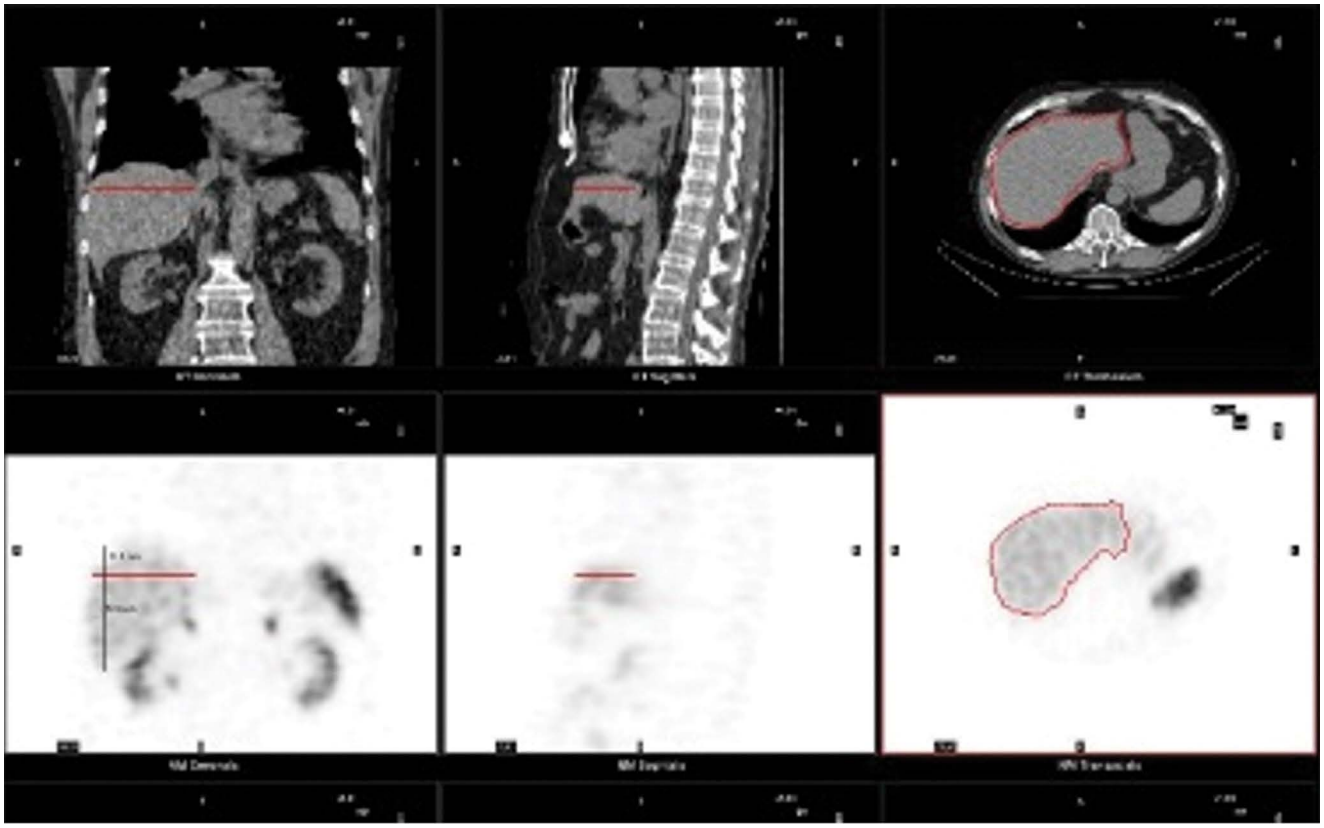

Figure 3. Medium liver volume of interest (VOI) — segmentation method 3

After completing the segmentation with each of the described methods, we calculated SUVbw max, SUVbm mean, SUVlbm max, and SUVlbm mean for each outlined VOI.

SUVbw and SUVlbm were calculated using the following formulas [13–15]:

$$SUV_{bw} = \frac{\text{SPECT image Pixels uptake (Bq/ml)} \times \text{weight (g)}}{\text{Actual activity}} \quad (1)$$

$$SUV_{lbm} = \frac{\text{SPECT image Pixels uptake (Bq/ml)} \times \text{LBM (kg)}}{\text{Actual activity} \times 1000} \quad (2)$$

where:
Actual activity: activity during scanning,

$$\text{pixels uptake} \quad (\text{Bq/ml}) = 37 \times 10^3 \times \frac{60}{\text{SPECTSensitivity (counts/min/}\mu\text{Ci)} \times \text{T (s)} \times \text{ml}} \quad (3)$$

where T-scan duration in seconds.
for males:

$$\text{LBM in kg} = 1.10 \times (\text{weight in kg}) - 120 \times \frac{(\text{weight in kg})}{(\text{height in cm})^2} \quad (4)$$

for females:

$$\text{LBM in kg} = 1.07 \times (\text{weight in kg}) - 148 \times \frac{(\text{weight in kg})}{(\text{height in cm})^2} \quad (5)$$

Data were processed using Statistica 13.1 software. The normality of data distribution for SUV was verified with the Shapiro-Wilk test at the significance level $\alpha = 0.05$. The normal range for SUVs for healthy livers was determined using the formula: normal range = (mean –2SD; mean +2SD).

Method for the determination of SUVs in the group with liver lesions

For images with numerous liver lesions, up to five abnormal hot spheres were segmented each time: with the lowest, moderate, and highest SUV. This method enabled the inclusion of the whole range of lesions, assuring also that the ones with relatively low uptake of the radiopharmaceutical were considered in the quantitative analysis.

Method for the determination of SUVs in other tissues

The spleen and the gluteus medius muscle have a relatively uniform distribution of radiopharmaceuticals in the tissues. The accumulation of radiopharmaceuticals by the gluteus medius is usually very low and may correspond with the background activity of the peripheral blood circulation. The accumulation of radiopharmaceuticals in the spleen is usually very high, and its value may correspond with that for hot lesions. Due to the individual differences of radiopharmaceutical accumulation in particular tissues, quantitative data on the physiological uptake of ^{99m}Tc-Tektrotyd by the spleen and the gluteus medius may be useful in the diagnostic interpretation of SUV measured in the liver.

We calculated the SUV spleen/SUV liver ratios in 42 patients and the SUV liver/SUV gluteus medius ratios in 38 patients (in 4 patients gluteus medius muscles were not visible in the SPECT/CT images). VOI in the spleen region was segmented based on SPECT

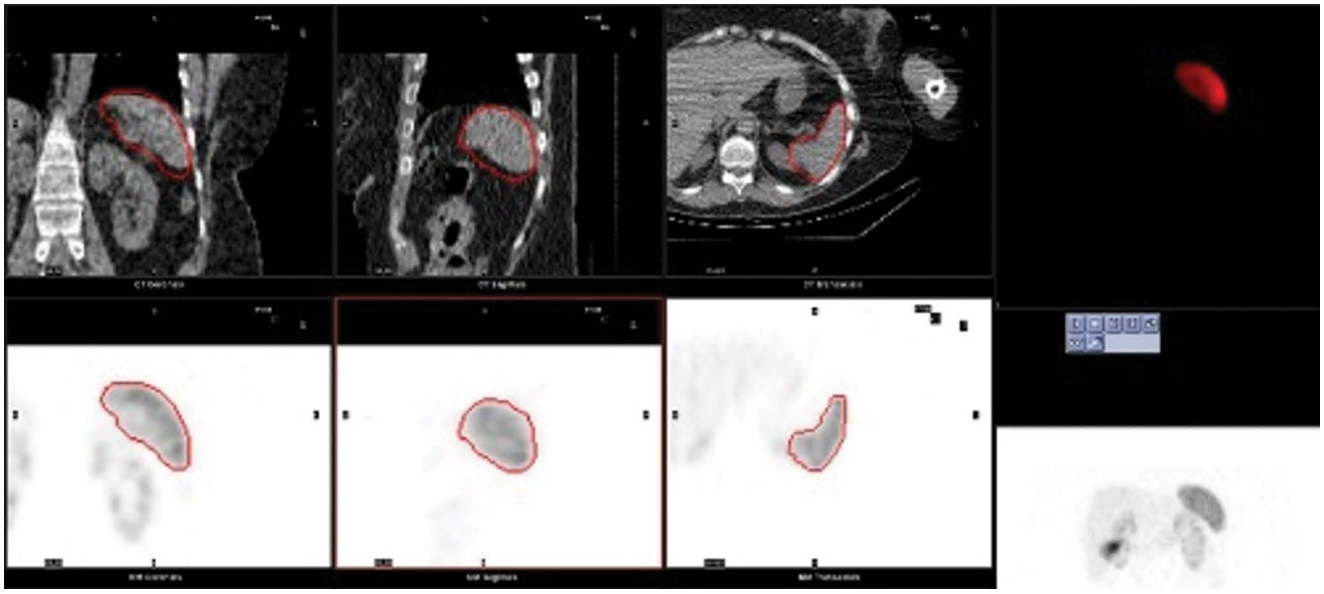

Figure 4. Segmentation of the spleen in single photon emission computed tomography (SPECT) slices

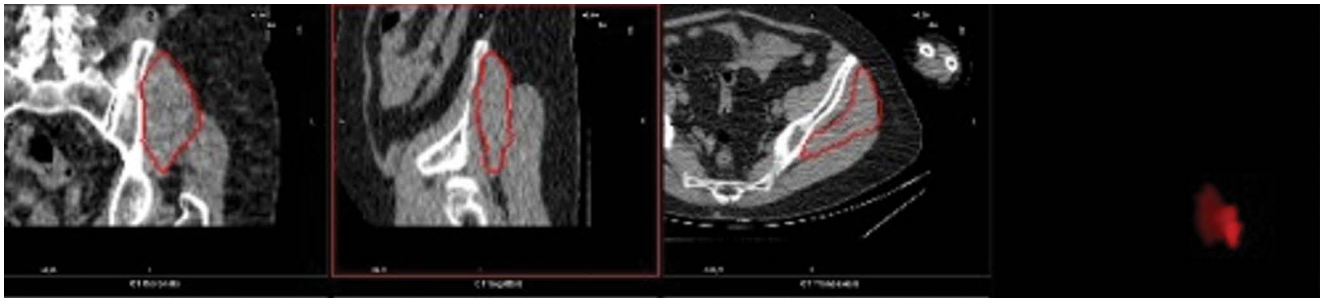

Figure 5. Segmentation of the gluteus medius muscle in computed tomography (CT) slices

and CT slices. VOI in the gluteus medius muscle was segmented based on CT slices. Figures 4 and 5 present the method for outlining VOI within the spleen and the gluteus medius muscle.

Estimation of the accuracy of SUV measurements

SPECT/CT acquisitions were performed using the National Electrical Manufacturers Association, International Electrotechnical Commission (NEMA IEC) Body Phantom with 6 hot spheres of different diameters: 10 mm, 13 mm, 17 mm, 22 mm, 28 mm, and 37 mm. The acquisition protocol and reconstruction parameters were identical to those used during imaging studies involving patients. SUVs are directly proportional to the activity concentration in the measured VOIs, and therefore the accuracy of the SUV measurement is closely related to the accuracy of the activity concentration measurement. Based on activity measurements performed with a calibrated activity meter and the results of image quantification, the relative standard error of mean activity concentration for VOIs in 6 spheres was determined. Figure 6 presents the segmentation of hot spheres in the NEMA IEC Body Phantom.

Results

Patients with healthy liver

1) Results of liver measurement

Results obtained for the quantification of SPECT/CT slices of healthy livers are presented in Table 1.

2) Results of measurements for the spleen and gluteus medius muscle

Table 2 presents SUVbw and SUVlbm for the spleen and gluteus medius muscle.

3) Standardized uptake value ratios: spleen/liver and liver/gluteus medius muscle

Table 3 presents normal ranges for SUV spleen/SUV liver ratios.

Table 4 presents normal ranges for SUV liver/SUV gluteus medius muscle ratios.

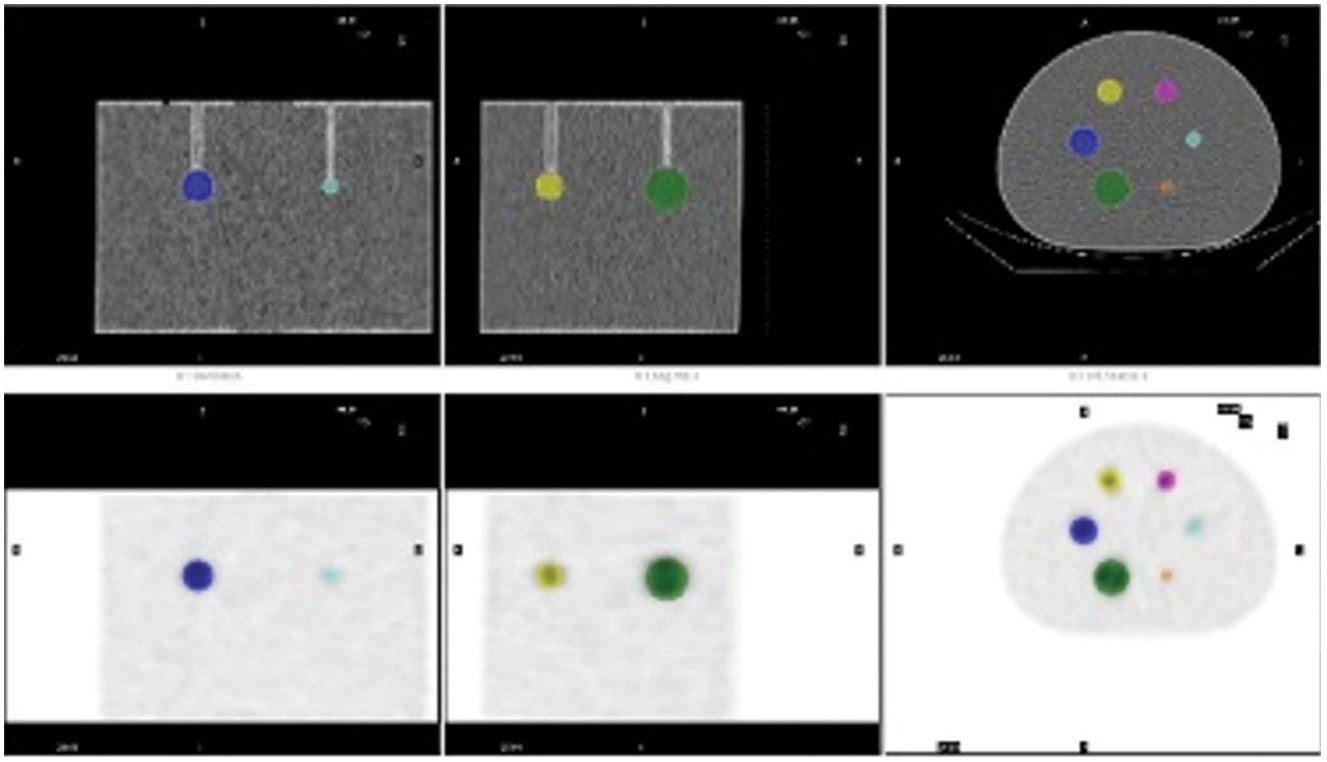

Figure 6. Segmentation of 6 hot spheres in the NEMA IEC Body Phantom; The RC — recovery coefficients curve was also plotted for hot spheres

Table 1. Standardized uptake value based on body weight **(**SUVbw) and standardized uptake value lean body mass (SUVlbm) measured in single photon emission computed tomography/ computed tomography (SPECT/CT) slices of healthy livers using three methods. The table presents normal ranges for SUVs for each segmentation method

	SUVbw max [g/mL]	SUVbw mean [g/mL]	SUVlbm max [g/mL]	SUVlbm mean [g/mL]
Method 1				
mean liver VOI: 1292.2 ± 299.1 mL				
Shapiro-Wilk test results	W = 0.96 p = 0.20	W = 0.95 p = 0.08	W = 0.98 p = 0.47	W = 0.98 p = 0.64
mean ± SD	12.6 ± 2.7	4.8 ± 1.3	8.4 ± 1.8	3.2 ± 0.8
minimum value–maximum value	7.7–19.0	2.5–9.1	4.4–11.5	1.5–4.8
normal range:	7.2–18.0	2.2–7.4	4.8–12.0	1.6–4.8
Method 2				
mean liver VOI: 2.5 ± 0.7 mL				
Shapiro-Wilk test results	W = 0.99 p = 0.86	W = 0.98 p = 0.58	W = 0.97 p = 0.23	W = 0.97 p = 0.28
mean ± SD	8.4 ± 2.3	5.8 ± 1.7	5.7 ± 1.4	4.0 ± 1.1
minimum value–maximum value	3.5–13.7	2.6–9.7	2.9–7.9	2.0–5.8
normal range:	3.8–13.0	2.4–9.2	2.9–8.5	1.8–6.2
Method 3				
mean liver VOI: 30.8 ± 7.7 mL				
Shapiro-Wilk test results	W = 0.99 p = 0.89	W = 0.94 p = 0.06	W = 0.97 p = 0.22	W = 0.98 p = 0.76
mean ± SD	9.6 ± 2.2	4.9 ± 1.3	6.5 ± 1.5	3.3 ± 0.9
minimum value–maximum value	4.9–15.2	2.6–9.4	2.3–9.1	1.5–5.0
normal range:	5.2–14.0	2.3–7.5	3.5–9.5	1.5–5.1

SD — standard deviation; SUVbw — standardized uptake value normalized to body weight; SUVlbm — standardized uptake value normalized to lean body mass; VOI — volume of interest

Table 2. Standardized uptake value based on body weight (SUVbw) and standardized uptake value lean body mass (SUVlbm) measured in single photon emission computed tomography/ computed tomography SPECT/CT slices of the spleen and gluteus medius muscle

	SUVbw max	SUVbw mean	SUVlbm max	SUVlbm mean
Spleen				
mean ± SD	39.3 ± 13.9	19.5 ± 4.4	26.22 ± 8.1	13.08 ± 3.0
mean volume: 236 ± 101 mL				
Gluteus medius				
mean ± SD	2.4 ± 0.7	0.5 ± 0.2	1.6 ± 0.5	0.4 ± 0.6
mean volume: 108 ± 34 mL				

SUVbw — standardized uptake value normalized to body weight; SUVlbm — standardized uptake value normalized to lean body mass

Table 3. Normal ranges for the standardized uptake value (SUV) spleen / standardized uptake value (SUV) liver ratios determined for each of the three segmentation methods and four standardized uptake values

	SUVbw max ratio	SUVbw mean ratio	SUVlbm max ratio	SUVlbm mean Ratio
Method 1				
mean ± SD	3.2 ± 0.9	4.2 ± 1.1	3.2 ± 0.9	4.2 ± 1.1
normal range:	1.4–5.0	2.0–6.4	1.4–5.0	2.0–6.4
Method 2				
mean ± SD	4.9 ± 1.5	3.6 ± 1.2	4.8 ± 1.4	3.4 ± 1.0
normal range:	1.9–7.9	1.2–6.0	2.0–7.6	1.4–5.4
Method 3				
mean ± SD	4.2 ± 1.2	4.1 ± 1.1	4.2 ± 1.2	4.1 ± 1.1
normal range:	1.8–6.6	1.9–6.3	1.8–6.6	1.9–6.3

SUVbw — standardized uptake value normalized to body weight; SUVlbm — standardized uptake value normalized to lean body mass

Table 4. Normal ranges for the SUV liver/SUV gluteus medius muscle ratios determined for each of the three segmentation methods and four SUVs

	SUVbw max ratio	SUVbw mean ratio	SUVlbm max ratio	SUVlbm mean ratio
Method 1				
mean ± SD	4.9 ± 1.5	3.6 ± 1.2	4.8 ± 1.4	3.5 ± 1.0
normal range:	1.9–7.9	1.2–6.0	2.0–7.6	1.5–5.5
Method 2				
mean ± SD	3.6 ± 1.1	13.1 ± 5.3	3.6 ± 1.1	12.9 ± 5.8
normal range:	1.4–5.8	2.5–23.7	1.4–5.8	1.3–24.5
Method 3				
mean ± SD	4.3 ± 1.3	11.2 ± 4.3	4.2 ± 1.3	10.8 ± 4.7
normal range:	1.7–6.9	2.6–19.8	1.6–6.8	1.4–20.2

SUVbw — standardized uptake value normalized to body weight; SUVlbm — standardized uptake value normalized to lean body mass

Patients with hot liver lesions

Quantitative analysis was performed for 58 lesions. The mean VOI for lesions was 22.7 ± 46.2 mL (range: 1.1–277.9 mL). 65% of the hot lesions had a volume greater than 5 mL.

Results obtained for the quantification of SPECT/CT slices of livers with hot lesions are presented in Table 5.

Estimation of the accuracy of SUV measurements

Relative errors of spheres' volume and activity concentration measurements obtained for SPECT/CT images of the NEMA IEC Body Phantom are presented in Table 6.

Figure 7 presents the RCmax (recovery coefficient curve) for the accuracy of spheres' activity concentration measurements in SPECT/CT images.

Discussion

Standardization of quantitative SPECT/CT is currently a crucial clinical problem. The feasibility of absolute quantification in SPECT/CT imaging was confirmed by different studies more than 10 years ago [16–19], but no standard quantification procedures, clinical analyses, or principles for the validation of equipment have been established to this day.

Table 5. Results of quantitative analysis of SPECT/CT slices of livers with hot lesions.

	SUVbw max	SUVbw mean	SUVlbm max	SUVlbm mean
Mean value [g/mL]	37.6 ± 27.1	21.0 ± 13.8	27.7 ± 20.3	15.5 ± 10.3
range [g/mL]	13.3–129.9	7.1–70.3	6.3–95.8	3.4–52.2

SUVbw — standardized uptake value normalized to body weight; SUVlbm — standardized uptake value normalized to lean body mass

Table 6. Relative errors of spheres' volume and activity concentration measurements. $Ac_{measured}$ — activity concentration measured with a dose calibrator was 255 kBq/mL.

	Vt	Vi	SE_{Vi}	$Ac_{in\ image}$ mean	$SE_{Ac\ in\ image}$
Sphere diameter [mm]	True sphere volume [mL]	Sphere volume in image [mL]	Relative standard error of volume [%]	Activity concentration mean in image [kBq/mL]	Relative standard error of activity concentration [%]
10	0.5	0.4	20.0	90	64.7
13	1.2	1.3	-8.3	130	49.0
17	2.6	2.3	11.6	199	22.0
22	5.6	5.0	10.7	226	11.4
28	11.5	10.7	6.9	237	7.1
37	26.5	25.7	3.0	240	5.9

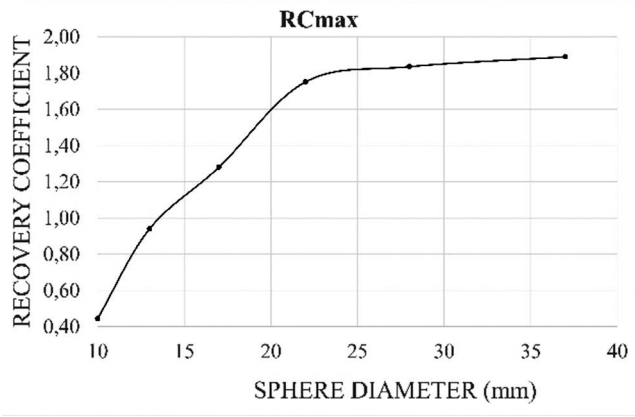

Figure 7. Recovery coefficient (RCmax) curve. Recovery coefficients were determined as the ratio of the maximum activity concentration measured in the image ($Ac_{in\ image}$ max) to the activity concentration measured with a dose calibrator ($Ac_{measured}$)

Determination of the normal range of SUVs in studies is difficult because of very significant differences in the uptake of different radiopharmaceuticals associated with several biological and physical factors [20]. Firstly, the pharmacokinetics of the injected radiopharmaceutical depends on the metabolism of the examined patient. Secondly, the images are acquired at different time points following the injection of the radiopharmaceutical because of the limited availability of the gamma camera. The calculation of SUV involves measurements obtained using two instruments — a gamma camera and an activity meter. Therefore, inaccurate calibration of either instrument may influence the level of accuracy in the SUV measurement. There are also other factors affecting the variability of SUV, including the quality of image reconstruction, the efficiency of corrections for the scatter and attenuation of radiation in the patient's tissues, and the limited resolution of gamma camera detectors, which create difficulties with the segmentation of selected regions of interest. Determination of absolute SUV is a complex task, but it is achievable [21].

A significant problem investigated in our study was to determine the optimal method for measuring SUV in healthy liver tissue. Method 1, which involved the segmentation of the entire liver region (except the extrahepatic bile ducts), although very laborious, seemed to be the most appropriate in the initial phase of analysis. The disadvantage of this method was the possibility of covering many intrahepatic bile ducts in a segmented large VOI (mean volume 1292 mL). Method 2 involved the segmentation of a small regular fragment of the liver (mean VOI: 2.5 mL) and was used because physicians prefer a technique that does not require a precise outlining of tissue contours for the estimation of SUVmax in ROI. The disadvantage of this method was the lack of reproducibility with respect to the anatomical location of the selected liver fragment in the examined patients. The position of the intervertebral disc between Th11 and Th12 may correspond to very different liver segments in different patients. Method 3, used in the presented study, was regarded by the authors as the optimal technique for VOI segmentation and the assessment of normal ranges for SUV. It allowed for reproducible localization of the medium VOI (with a mean volume of 31 mL) within liver segments VII and VIII (in transverse SPECT slices from different patients), based on the dimensional analysis of its coronal and sagittal CT slices.

All mean values of SUVbw max, SUVbw mean, SUVlbm max, and SUVlbm mean calculated for hot liver lesions in the "pathological group' were several times higher than the upper limits of normal ranges for SUVs obtained with all methods.

The effect of biological and physical factors on the variability of SUV (different biokinetics of the radiopharmaceutical in patients, different time intervals between the injection and start of SPECT/CT acquisition) can be limited by using relative SUV ratios: SUV spleen/SUV liver and SUV liver/SUV gluteus medius muscle. Normal ranges for SUV spleen/SUV liver ratios calculated in our

study have lower variance (an average of 19%) compared to normal ranges for SUV liver. The variance of the mean normal range for the SUV liver/SUV gluteus medius ratio has the same feature, except for SUVmean estimated.

Phantom validation revealed good accuracy (maximum relative SE ~ 11%) of the volume and concentration measurement in hot spheres with diameters: 22, 28, and 37 mm (VOI 5.6, 11.5, and 26.5 mL, respectively). The clinical results for the accuracy of concentration measurements obtained in our study for the three largest spheres were consistent with the results reported by the GE Healthcare laboratory [13]. The accuracy of the activity concentration measurement for a sphere with a 17 mm diameter (volume 2.6 mL) in our study was 8% lower than the accuracy obtained by the GE Healthcare laboratory. SUVs calculated for hot liver lesions with volumes smaller than 5 mL are biased with a significant measurement error.

The shape of RCmax corresponds with recovery coefficients reported by other researchers [21–23].

Conclusions

Segmentation in the mid-coronal CT image, at one-fourth of the height of the liver measured from the top, with a medium-sized VOI outlined on a given transverse SPECT slice was regarded as the optimal method for estimating normal ranges for standardized uptake values.

It is necessary to standardize quantification methods in the SPECT/CT studies. Our work is a step forward in obtaining standardization of SPECT/CT SUV calculation methods.

Calculations for radiopharmaceutical uptake in tumors with volumes smaller than 5 mL are biased with a significant measurement error.

Availability of data and material

The datasets generated during and/or analyzed during the current study are available from the corresponding author on reasonable request.

Authors' contributions

All authors contributed to the study's conception and design. Material preparation, data collection and analysis were performed by Sara Kurkowska, Hanna Piwowarska-Bilska and Bozena Birkenfeld. The first draft of the manuscript was written by Hanna Piwowarska-Bilska and all authors commented on previous versions of the manuscript. All authors read and approved the final manuscript.

Ethics approval and consent to participate

Ethical approval was waived by the local Ethics Committee of Pomeranian Medical University in view of the retrospective nature of the study and all the procedures being performed were part of the routine care.

Conflict of interest

The authors declare that they have no competing interests.

References

1. Schillaci O, Spanu A, Palumbo B, et al. SPECT/CT in neuroendocrine tumours. Clin Transl Imaging. 2014; 2(6): 477–489, doi: 10.1007/s40336-014-0091-x.
2. Sharma P, Singh H, Bal C, et al. PET/CT imaging of neuroendocrine tumors with (68)Gallium-labeled somatostatin analogues: An overview and single institutional experience from India. Indian J Nucl Med. 2014; 29(1): 2–12, doi: 10.4103/0972-3919.125760, indexed in Pubmed: 24591775.
3. Gabriel M, Decristoforo C, Donnemiller E, et al. An intrapatient comparison of 99m Tc-EDDA/HYNIC-TOC with 111 In-DTPA-octreotide for diagnosis of soma-tostatin receptor-expressing tumors. J Nucl Med. 2003; 44(5): 708–16, indexed in Pubmed: 12732671.
4. Briganti V, Cuccurullo V, Berti V, et al. Tc-EDDA/HYNIC-TOC is a New Opportunity in Neuroendocrine Tumors of the Lung (and in other Malignant and Benign Pulmonary Diseases). Curr Radiopharm. 2020; 13(3): 166–176, doi: 10.2174/1874471013666191230143610, indexed in Pubmed: 31886756.
5. Artiko V, Sobic-Saranovic D, Pavlovic S, et al. The clinical value of scintigraphy of neuroendocrine tumors using (99m)Tc-HYNIC-TOC. J BUON. 2012; 17(3): 537–542, indexed in Pubmed: 23033296.
6. Trogrlic M, Težak S. Incremental value of Tc-HYNIC-TOC SPECT/CT over whole-body planar scintigraphy and SPECT in patients with neuroendocrine tumours. Nuklearmedizin. 2017; 56(3): 97–107, doi: 10.3413/Nukmed-0851-16-10, indexed in Pubmed: 28164207.
7. Yamaga LY, Neto GC, da Cunha ML, et al. 99mTc-HYNIC-TOC increased uptake can mimic malignancy in the pancreas uncinate process at somatostatin receptor SPECT/CT. Radiol Med. 2016; 121(3): 225–228, doi: 10.1007/s11547-015-0593-2, indexed in Pubmed: 26558391.
8. Boellaard R, O'Doherty MJ, Weber WA, et al. FDG PET and PET/CT: EANM procedure guidelines for tumour PET imaging: version 1.0. Eur J Nucl Med Mol Imaging. 2010; 37(1): 181–200, doi: 10.1007/s00259-009-1297-4, indexed in Pubmed: 19915839.
9. European Medicines Agency. Assesment report. SomaKit TOC International non-proprietary name: edotreotide Procedure No. EMEA/H/C/004140/0000. EMA/734748/2016 Committee for Medicinal Products for Human Use (CHMP). 2016.
10. Krenning EP, Bakker WH, Breeman WA, et al. Localisation of endocrine-related tumours with radioiodinated analogue of somatostatin. Lancet. 1989; 1(8632): 242–244, doi: 10.1016/s0140-6736(89)91258-0, indexed in Pubmed: 2563413.
11. Hope TA, Calais J, Zhang Li, et al. 111 In-Pentetreotide Scintigraphy Versus Ga-DOTATATE PET: Impact on Krenning Scores and Effect of Tumor Burden. J Nucl Med. 2019; 60(9): 1266–1269, doi: 10.2967/jnumed.118.223016, indexed in Pubmed: 30850506.
12. Beck M, Sanders JC, Ritt P, et al. Longitudinal analysis of bone metabolism using SPECT/CT and (99m)Tc-diphosphono-propanedicarboxylic acid: comparison of visual and quantitative analysis. EJNMMI Res. 2016; 6(1): 60, doi: 10.1186/s13550-016-0217-4, indexed in Pubmed: 27464623.
13. NM Quantification. Q.Metrix for SPECT/CT Package. White Paper, DOC1951185, GE Healthcare 2017.
14. Kim CK, Gupta NC, Chandramouli B, et al. Standardized uptake values of FDG: body surface area correction is preferable to body weight correction. J Nucl Med. 1994; 35(1): 164–167, indexed in Pubmed: 8271040.
15. Sugawara Y, Zasadny KR, Neuhoff AW, et al. Reevaluation of the standardized uptake value for FDG: variations with body weight and methods for correction. Radiology. 1999; 213(2): 521–525, doi: 10.1148/radiology.213.2.r99nv37521, indexed in Pubmed: 10551235.
16. Zeintl J, Vija AH, Yahil A, et al. Quantitative accuracy of clinical 99mTc SPECT/CT using ordered-subset expectation maximization with 3-dimensional resolution recovery, attenuation, and scatter correction. J Nucl Med. 2010; 51(6): 921–928, doi: 10.2967/jnumed.109.071571, indexed in Pubmed: 20484423.

17. Vandervoort E, Celler A, Harrop R. Implementation of an iterative scatter correction, the influence of attenuation map quality and their effect on absolute quantitation in SPECT. Phys Med Biol. 2007; 52(5): 1527–1545, doi: 10.1088/0031-9155/52/5/020, indexed in Pubmed: 17301469.
18. Willowson K, Bailey DL, Baldock C. Quantitative SPECT reconstruction using CT-derived corrections. Phys Med Biol. 2008; 53(12): 3099–3112, doi: 10.1088/0031-9155/53/12/002, indexed in Pubmed: 18495976.
19. Shcherbinin S, Celler A, Belhocine T, et al. Accuracy of quantitative reconstructions in SPECT/CT imaging. Phys Med Biol. 2008; 53(17): 4595–4604, doi: 10.1088/0031-9155/53/17/009, indexed in Pubmed: 18678930.
20. Huang SC. Anatomy of SUV. Standardized uptake value. Nucl Med Biol. 2000; 27(7): 643–646, doi: 10.1016/s0969-8051(00)00155-4, indexed in Pubmed: 11091106.
21. Peters SMB, van der Werf NR, Segbers M, et al. Towards standardization of absolute SPECT/CT quantification: a multi-center and multi-vendor phantom study. EJNMMI Phys. 2019; 6(1): 29, doi: 10.1186/s40658-019-0268-5, indexed in Pubmed: 31879813.
22. Gnesin S, Leite Ferreira P, Malterre J, et al. Phantom Validation of Tc-99m Absolute Quantification in a SPECT/CT Commercial Device. Comput Math Methods Med. 2016; 2016: 4360371, doi: 10.1155/2016/4360371, indexed in Pubmed: 28096891.
23. Collarino A, Pereira Arias-Bouda LM, Valdés Olmos RA, et al. Experimental validation of absolute SPECT/CT quantification for response monitoring in breast cancer. Med Phys. 2018; 45(5): 2143–2153, doi: 10.1002/mp.12880, indexed in Pubmed: 29572848.